JOURNAL OF MATERIALS SCIENCE 25 (1990) 2705–2710

Kinetics of phase separation and thermal behaviour of gel-derived Al_2O_3 doped by Cr_2O_3: an X-ray diffraction and fluorescence spectroscopy study

G. CARTURAN*, R. DI MAGGIO*, M. MONTAGNA‡, O. PILLA‡, P. SCARDI*
*Dipartimento di Ingegneria, Universita' di Trento, 38050 Mesiano, Trento, Italy
‡Dipartimento di Fisica, Universita' di Trento, 38050 Povo, Trento, Italy

Alpha-alumina crystallization from boehmite obtained from a gel was studied as a function of heating temperature and residence time. X-ray analysis allowed the determination of phases and their crystallite size; fluorescence spectroscopy was also studied as a complementary identification technique. The results reveal the general behaviour of gel-derived Al_2O_3 phases and their transformation. The occurrence of an amorphous intermediate state was ruled out.

1. Introduction

The sol–gel route is a suitable approach to the synthesis of Al_2O_3 for important applications such as the manufacture of basic products for high-value ceramics [1] and fibres [2–5]. Studies have shown that thermal treatment of the gel affords some irreversible phase transitions, a unique phase being associated with a definite temperature interval. The following scheme has been proposed to describe Al_2O_3 gel evolution with temperature [6]:

$$\text{Pseudo-boehmite} \xrightarrow{400^\circ C} \text{Amorphous} \xrightarrow{600^\circ C} \delta \xrightarrow{1000^\circ C} \theta \xrightarrow{1200^\circ C} \alpha$$

This scheme refers to gel-derived Al_2O_3 samples prepared with a single heating rate, disregarding possible effects of preparative details, ageing and phase stabilization for long-term treatments at intermediate temperatures.

In order to standardize the synthesis of α-alumina by the gel method, it seems useful to have a more precise definition of the stability interval of the individual Al_2O_3 phases by performing a systematic study of the behaviour of gel-derived Al_2O_3 taking into account both heating temperature and residence time. The expectation is that some Al_2O_3 phases may overlap their stability intervals owing to analogous thermodynamic contents, although their occurrence may involve different kinetics [7, 8].

The assessment of an amorphous phase as first product of pseudo-boehmite disappearance may also require a more detailed investigation. Indeed, the occurrence of this amorphous state may rule the kinetics of the entire process. δ-Al_2O_3, χ-Al_2O_3, θ-Al_2O_3, and κ-Al_2O_3 phases, observed at intermediate temperatures before α-Al_2O_3 occurrence, may be derived from a single precursor leading to various Al_2O_3 forms depending on crystallization conditions. In addition, different gelling condition may afford different hydroxides which, as for natural aluminium hydroxides, may find variable intermediate phases before collapsing to α-Al_2O_3 [9]. Thus, for better understanding of Al_2O_3 crystallization it is promising to ascertain the occurrence and stability interval of the amorphous state, and the role of gel preparation procedures.

The present work uses wide-angle X-ray diffraction (XRD) analysis and optical fluorescence spectroscopy for phase characterization of Cr_2O_3-doped Al_2O_3 gel. Cr^{3+} ion provide important coordination and structural information by means of fluorescence spectroscopy [10]. The combination of these techniques has recently been reported by Hirai *et al.* [6] in a study of gel-derived Al_2O_3; our work extends that study with special attention to the kinetics of the crystallization processes. As a first approximation the role of Cr^{3+} in promoting alumina nucleation was disregarded; a further investigation on the possible influence of Cr^{3+} on preferential crystallization will be the object of a future study.

2. Experimental procedure

2.1. Preparation of samples by the sol–gel method and thermal treatment

Samples with 0.1 mol % Cr_2O_3 were obtained by evaporation and calcination of an alumina sol. This sol was prepared as described by Yoldas [11]. In a typical experiment, aluminium iso-propoxide (100 g) and chromium acetylacetonate (0.17 g) were added to 400 ml of deionized H_2O. After heating for 1 h at 80° C, concentrated HNO_3 (1.5 ml) was added; the system was left aside at 100 to 110° C for about one day. The reaction mixture was cooled to room temperature, producing a milky sol. The gel was then exchanged with water and subsequently dried at 95° C. This procedure had the effect of strongly reducing the

0022–2461/90 $03.00 + .12

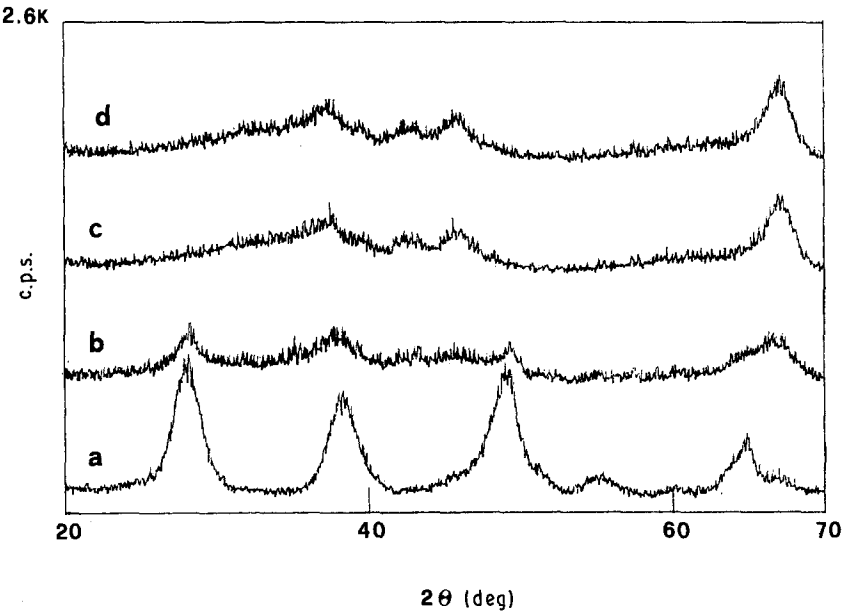

Figure 1 X-ray diffraction spectra of samples (a) AL 170, (b) AL 440, (c) AL 518 and (d) AL 600.

luminescence spectra of a broad-band contribution due to residual organic groups. The powders thus obtained were divided into various batches for successive ageing and thermal treatments. The samples were heated at 4° C min^{-1} up to various temperatures as reported in Table I. In some cases water-exchange was avoided, and samples were directly heated as previously described.

2.2. X-ray diffraction analysis

Powdered samples were examined in the reflection mode with a Rigaku D/max-B diffractometer with a scintillation counter and a graphite curved-crystal monochromator in the diffracted beam. Each measurement was carried out at 1 deg min^{-1} with a step of 0.02 deg, corresponding to 1.2 sec per step. All samples were analysed at 45 kV and 40 mA in the range $20° \leqslant 2\theta \leqslant 70°$. A Casio 6000 computer was employed for data processing; besides the routine operation of background reduction, smoothing and peak-search, phase identification was carried out by means of a search–match program provided together with JCPDS cards [12]. Profile analysis was carried out for samples treated at 1200° C. Line-broadening analysis was performed following the Warren–Averbach method [13] applied to 0 1 2 and 0 2 4 peaks of α-Al_2O_3, and employing a KCl sample as standard for instrumental peak determination. For the other samples, where a complex overlap between peaks of the various phases occurred, the Scherrer formula was employed, together with a computer program for peak separation.

TABLE I Sample treatments

Sample	Temperature (° C)	Ageing time
AL 170	170	12 h
AL 440	440	2 h
AL 518	518	2 h
AL 518a	518	5 min
AL 518b	518	12 h
AL 600	600	2 h
AL 800	800	2 h
AL 800a	800	5 min
AL 800b	800	12 h
AL 1000	1000	2 h
AL 1200	1200	2 h
AL 1200a	1200	5 min
AL 1200b	1200	20 min

2.3. Fluorescence spectroscopy

Fluorescence spectra were taken by exciting with an HeNe or argon ion laser, emission being dispersed by a Jobin–Yvon HRS4 monochromator. Time-resolved spectra and lifetimes were recorded by mechanically chopping the laser light, which gave a time resolution of 80 μsec. The excitation spectra were obtained by tungsten lamp plus monochromator excitation.

3. Results and discussion

The Al_2O_3 gel was kept at 170° C for 24 h, ensuring the removal of solvent and organic radicals, as verified by means of differential thermal analysis. A weight loss between 250 and 450° C, corresponding to the virtually quantitative removal of H_2O from pseudo-boehmite, was found. Table I lists the samples examined and their thermal treatments.

Fig. 1 shows the X-ray spectrum evolution for samples treated for 2 h at temperatures in the range 170 to 600° C. This heating interval was monitored with particular care in order to determine the structural evolution of boehmite and the stability interval of a possible amorphous state. The product as prepared at 170° C shows the boehmite structure with an average dimension of crystallites of 5 nm. After 2 h at 440° C (Fig. 1b) the X-ray spectrum of the material was not suitable for immediate interpretation. Boehmite peaks were still recognizable but were weaker and broader than those observed for the product at 170° C. Other peaks may be attributed to microcrystallites of alumina phases other than boehmite. Peak broadness prevented definite phase identification, even for the sample kept at 518° C for 2 h (Fig. 1c), although the boehmite had completely disappeared. A tentative assignment to δ-Al_2O_3 and χ-Al_2O_3 is proposed: in the first case a good agreement is found between peak positions and relevant intensity ratios, whereas χ-Al_2O_3 occurrence

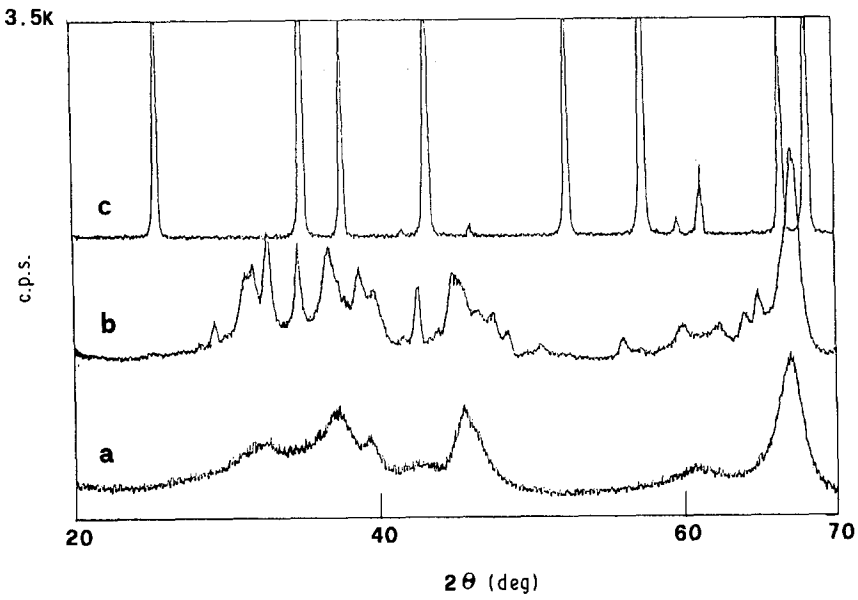

Figure 2 X-ray diffraction spectra of samples (a) AL 800, (b) AL 1000 and (c) AL 1200.

is supported by the presence of the peak at $2\theta = 43°$. Among the aluminas stable at moderately low temperatures, only χ-Al_2O_3 shows this peak. Prolonged heating at 518° C for 10 h or at 600° C for 2 h does not affect relevant X-ray spectra (Fig. 1d): the absence of any evolution with respect to the sample maintained at 518° C for only 2 h (Al 518) enlarges the field of coexistence between χ-Al_2O_3 and δ-Al_2O_3. The complex overlapping of peaks attributable to the χ and δ phases is observed even for the sample heated at 800° C for 2 h (Fig. 2a). In this case more details are recognized because of peak sharpening, owing to better crystallization. On the other hand, the spectrum remains virtually unchanged on increasing the ageing time up to 12 h at the same temperature.

These data, collected for different ageing times in the interval 440 to 800° C, do not show any amorphous transition state produced by the disappearance of boehmite [6]; on the contrary our results can be accounted for by boehmite collapse to δ-Al_2O_3 nucleation, followed by a moderate size increase upon further thermal treatments.

After a thermal treatment for 2 h at 1000° C, sample AL 1000 appeared to be constituted only of θ-Al_2O_3 and κ-Al_2O_3 (Fig. 2b): peak attribution is quite reliable owing to the good resolution, although (due to the background noise of the spectrum) nucleation of α-Al_2O_3 or the residual presence of δ-Al_2O_3 cannot be excluded. Actually, the presence of α-Al_2O_3 nuclei was foreseen since α-Al_2O_3 is detected by ageing at 1000° C for 10 h. Grain sizes determined according to the Scherrer approximation were 13 and 24 nm for θ-Al_2O_3 and κ-Al_2O_3, respectively. Heating at 1200° C for 2 h or for longer, up to 12 h, only produces α-Al_2O_3 (Fig. 2c).

Samples not exchanged with water display different behaviour: χ- and κ-Al_2O_3 phases were never observed, suggesting the invaluable effect of water content in determining the structural evolution of Al_2O_3 gel.

The importance of residence time is evident on analysing the phase evolution occurring at 1200° C. Fig. 3 shows the spectra of samples prepared at 1200° C for different ageing times. After a few minutes at 1200° C (Fig. 3a) the detectable phase is δ-Al_2O_3, but a 20 min ageing is sufficient to modify the microstructure with the formation of α-, θ- and κ-Al_2O_3 (Fig. 3b). At this stage the contribution of α-Al_2O_3 is the most important, although the crystallite size is

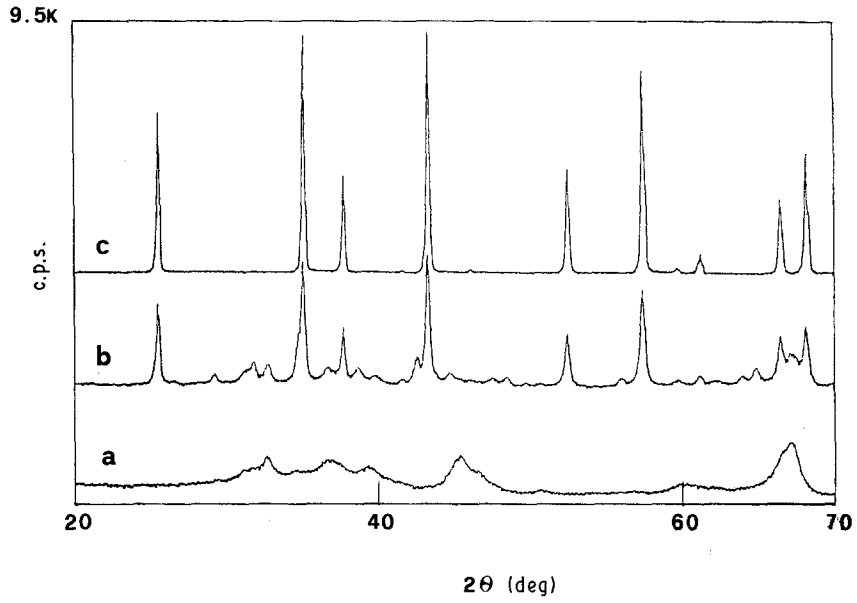

Figure 3 X-ray diffraction spectra of samples (a) AL 1200b, (b) AL 1200c and (c) AL 1200.

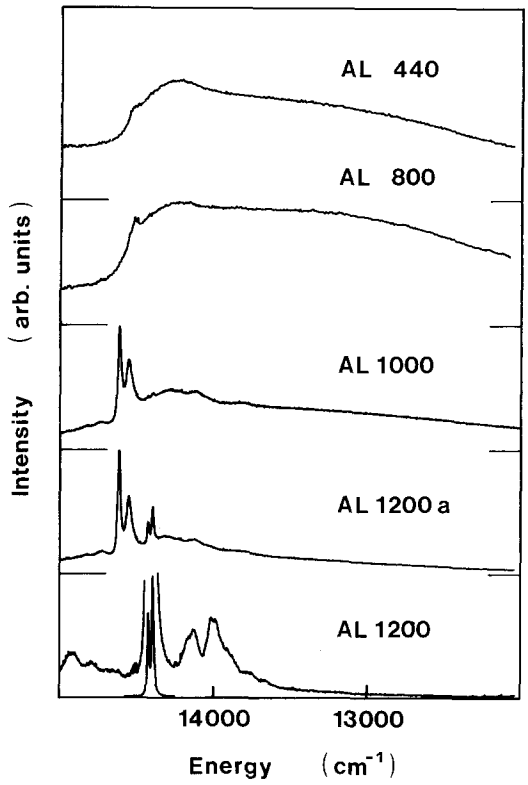

Figure 4 Room-temperature emission spectra of several samples under 632.8 nm excitation. Traces are labelled following Table I. The intensity of the doublet (lower trace) was divided by a factor of 20.

smaller than for the sample heated for 2 h (Fig. 3c). The evaluation of crystallite dimensions for samples treated at 1200° C for 20 min (AL 1200b) and 2 h (AL 1200) was performed by the Scherrer and Warren–Averbach approaches. In the absence of well-shaped pure crystalline standards of χ-, θ-, and κ-Al_2O_3, only the crystallite dimensions of α-Al_2O_3 were measured and compared; the values obtained are reported in Table II. The agreement of the results is worthy of note, taking into account that the Scherrer formula is expected to give overestimated values, especially for well crystallized and slightly strained systems.

Most samples identified by X-ray analysis were studied by fluorescence spectroscopy. Fig. 4 shows the room-temperature fluorescence spectra under 623.8 nm excitation for the set of samples heated for 2 h at different temperatures. Sample AL 1200, aged for 2 h at 1200° C, shows the characteristic emission spectrum of ruby (chromium-doped α-alumina) in agreement with X-ray results. The spectrum is dominated by R1 and R2 lines arising from the transition from the first excited level ^2E, split by 29 cm^{-1} in the case of trigonal distortion [14, 17], to the ground state $^4A_2$. In addition to the R-zero phonon lines, weaker structures due to their relative sidebands may also be observed.

TABLE II Mean dimension of crystallites of α-Al_2O_3 heated at 1200° C for 20 min and 2 h

Calculation method	Mean dimension (nm)	
	AL 1200b	AL 1200
Warren–Averbach	60	110
Scherrer	90	> 200

As regards samples prepared at lower temperatures, direct assignment of the observed luminescences is not possible since, to out knowledge, the spectroscopy of Cr^{3+} ions in alumina phases other than α has never been studied in detail. However, comparison of the spectra offers valuable evidence of structural evolution.

For annealing temperatures in the range 400 to 800° C the luminescence spectrum consists of broad, featureless bands extending from 14 500 to 12 000 cm^{-1}. At higher annealing temperatures, several structures appear and broad-band contributions decrease. All the observed features are due to Cr^{3+} luminescence, as can be verified from their excitation spectra characterized by two strong bands arising from the $^4A_2 \rightarrow {}^4T_2$ and $^4A_2 \rightarrow {}^4T_1$ Cr^{3+} transitions in octahedral environments.

The broad band extending down to 12 000 cm^{-1}, which decreases in intensity on increasing the annealing temperature, is short-lived (lifetime < 0.1 m sec). On the contrary the structures between 14 500 and 14 000 cm^{-1}, which gain intensity on increasing the annealing temperature, are sharper and long-lived (lifetime in the 1 to 9 m sec range). The observation of broad bands together with sharp structures with different lifetimes is not surprising. In octahedral coordination the ground state of Cr^{3+} is $^4A_2$, while the first excited state may be ^2E or $^4T_2$ depending on the strength of the crystal field. According to the diagrams of Tanabe and Sugano [16, 17] the ^2E excited state is weakly affected by the crystal field and the $^2E \rightarrow {}^4A_2$ transition is a sharp zero phonon line and has phonon satellites. The $^4A_2 \rightarrow {}^2E$ transition is spin-forbidden but is partially allowed by ^2E–$^4T_2$ spin-orbit mixing and its lifetime may be very long (tens of milliseconds). At weak crystal field, the $^4T_2$ level may be lower in energy than ^2E so that fluorescence is due to the spin-allowed $^4T_2 \rightarrow {}^4A_2$ transition; this is a broad vibronic band extending to the near infrared, with a lifetime of the range of tens to hundreds of microseconds.

In a disordered system, the whole of the above situation may be found at different sites. For example, in glasses [18, 19] the $^2E \rightarrow {}^4A_2$ emission line is observed together with a $^4T_2 \rightarrow {}^4A_2$ broad band peaked at lower energies and deriving from weak crystal-field centres. The $^2E \rightarrow {}^4A_2$ line is broadened by disorder and shows a wide distribution of lifetimes. The contribution of ions in different sites can thus be selected by means of time-resolved spectroscopy or selective excitation.

In this regard, the emission of samples AL 440 and AL 800 (Fig. 4) is found to be composed of a broad ^2E structure around 14 200 cm^{-1}, whose excitation spectrum is characteristic of a high crystal field and very distorted centres, as usually observed in highly disorded systems. On the other hand, in these samples low crystal-field centres also occur. In fact, in the excitation spectra of the low-energy tail of the emission at about 12 500 cm^{-1}, where lifetimes less than 0.1 m sec are measured, the $^4T_2$ excitation band is very broad and shifted towards low energies. The $^4T_2$ low-energy tail extends below 14 000 cm^{-1} in the ^2E region, indicating that, for these Cr^{3+} ions, the $^4T_2$ level is the first excited one.

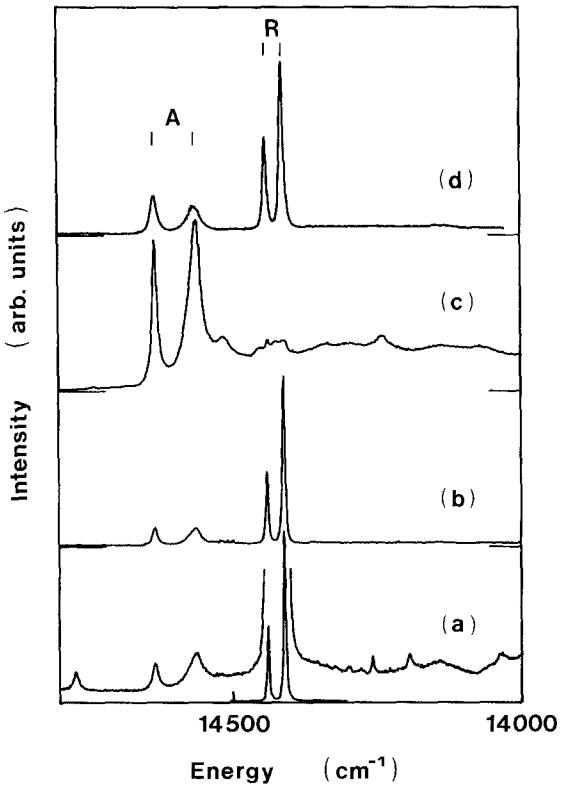

Figure 5 Details of emission spectra in the energy range of R and A lines at 77 K: (a) sample AL 1200; (b) sample AL 1200b; (c, d) sample AL 1200a. Excitation line: 632.8 nm for spectra (a), (b) and (c); 514.5 nm for spectrum (d). The intensity of the doublet (lower trace) was divided by a factor of 20.

Samples AL 1000 AL 1200a show sharp, long-lived features in their emission spectra (Fig. 4), assigned to Cr^{3+} ions in high crystal-field sites as verified by excitation spectroscopy. At the present time we cannot attempt assignment of the observed chromium-related emission to definite sites of definite transition-alumina phases.

Fig. 5 shows in detail the last steps of crystalline evolution towards the α-phase. The major features of all spectra in Fig. 5 are the two doublets A and R. By increasing either annealing temperature or heating time, the R lines of α-alumina gradually increase, being practically the only observable feature in the emission spectra (Fig. 5a). The A doublet arises from a site in a phase different than that of α-Al_2O_3. It dominates the spectrum (Fig. 5c) and gradually disappears with ageing at 1200° C.

The level of sensitivity which can be attained in a fluorescence measurement in detecting the presence of very diluted phases is also shown in Fig. 5. For instance, in the X-ray spectrum of sample AL 1200 only the α-phase is detected (Fig. 3c), while in Fig. 5a the A lines still occur, indicating that complete crystallization in the α-phase has not yet taken place. This fact underlines the much higher analytical power of spectroscopic analysis in comparison with X-ray phase identification. Moreover, the analytical power of optical spectroscopy can be increased since by varying the excitation line, the sensitivity to the emission of an individual phase may be increased. This is shown in Figs 5c and d where a drastic variation in the relative intensity of the A and R doublets is obtained only by changing the exciting line from 632.8 to 514.5 nm,

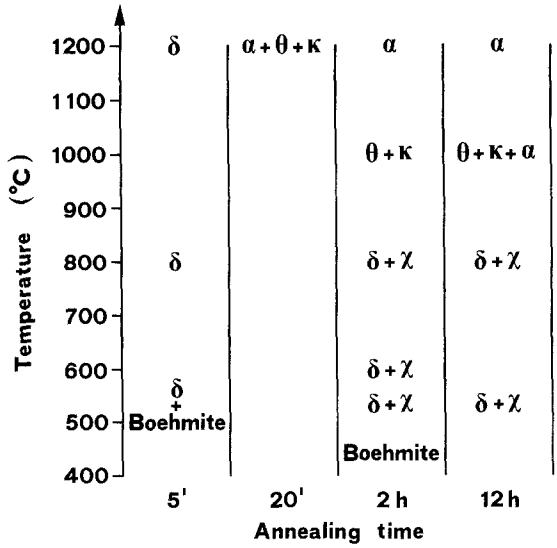

Figure 6 Diagram of Al_2O_3 phases, for H_2O-exchanged samples, at various temperatures and times.

respectively. With this same experimental method we also observed nucleation of α-alumina in sample AL 1000, heated for 2 h at 1000° C (Fig. 4). The identification of this phase is based on the appearance, in the emission spectrum under 514.5 nm excitation, of weak but detectable R-lines of chromium in α-alumina. It is worthy of note that, for the same sample, X-ray data give a structure composed only of θ- and κ-Al_2O_3 (Fig. 2b).

Fluorescence spectroscopy can be used as a complementary method for crystallite size analysis. Thus, the linewidth of the R-lines at 77 K decreases with increasing annealing temperature (Table III). After 2 h at 1200° C (AL 1200) the width of the R lines is roughly a factor of two larger than in ruby crystals of the same chromium concentration. The larger linewidth reflects the presence of an important degree of disorder on the Cr^{3+} sites in α-alumina. The narrowing of the R lines with annealing may be due to size effects. A progressive increase in the average crystalline size, as observed by X-ray analysis (Table II), should reduce grain-surface effects: in fact, the grain surface is seen as a defect by the neighbouring chromium impurities.

As regards the linewidths of the A lines (Table III), a decrease is observed on going from 1000 to 1200° C. However, longer treatments at 1200° C with progressive growth of the α phase do not cause any further narrowing. Since A lines are associated with an Al_2O_3 phase different from α-alumina, these results confirm the possible presence at 1200° C of phases other than α-Al_2O_3: indeed, a broadening is observed in sample

TABLE III Full-width-half-maximum (FWHM) of R and A lines at 77 K

Sample	FWHM (cm^{-1})*			
	Γ(R1)	Γ(R2)	Γ(A1)	Γ(A2)
AL 1000	–	–	55	16
AL 1200a	7	7	23	10
AL 1200b	5	5	21	10
AL 1200	4	4	25	11

*R1, 14418 cm^{-1}; R2, 14447 cm^{-1}; A1, 14572 cm^{-1}; A2, 14642 cm^{-1}.

AL 1200, where there are very few domains still not crystallized as the α-phase.

4. Conclusion

In conclusion, our results indicate that an intermediate amorphous state cannot be proposed for the pseudo-boehmite transformation to Al_2O_3, which involves the possible occurrence of various crystalline phases. Taking into account the heating temperatures and residence times, the resulting picture of Al_2O_3 phases obtained is shown in Fig. 6. This general scheme may be further complicated by the experimental preparation procedure: water content was found to favour the appearance of χ and κ phases for temperatures in the range 440 to 1000° C.

Acknowledgements

This work was partially supported by the Italian Ministero Della Pubblica Istruzione and by SNIA Fibre spa Milano, Italy.

References

1. L. G. KLEIN, "Sol–gel technology for thin films, fibres preforms, electronics and specialty shapes" (Noyes, New Jersey, 1988).
2. S. HORIKIRI, *Seramikkusu* **19** (1984) 194.
3. K. KAMIYA, S. SAKKA and N. TASHIRO, *Yogyo-Kyokai-Shi* **84** (1976) 614.
4. D. D. JOHNSON and H. J. SOWMAN, *Ceram. Eng. Sci. Proc.* **6** (1985) 1221.
5. T. MAK and S. SAKKA, *J. Non-Cryst. Solids* **100** (1988) 303.
6. Y. HIRAI *et al.*, *Solid State Commun.* **62** (1987) 637.
7. F. W. DYNYS, M. L. JUNBERG and J. W. HALLORAN, *Mater. Res. Soc. Symp. Proc.* **32** (1984) 321.
8. T. ASSIH *et al.*, *J. Mater. Sci.* **23** (1988) 3326.
9. W. W. GITZEN (Ed), "Alumina as a ceramic material" (American Physical Society, Columbus, 1970).
10. C. P. POOLE, *J. Phys. Chem. Solids* **25** (1964) 1169.
11. B. E. YOLDAS, *Ceram. Bull.* **54** (1975) 289.
12. JCPDS File (International Centre of Diffraction Data, Swarthmore, Pennsylvania, USA).
13. H. P. KLUG and L. E. ALEXANDER, "X-ray diffraction procedures" (Wiley, New York, 1974) pp. 643–655.
14. S. SUGANO and Y. TANABE, *J. Phys. Soc. Jpn* **13** (1958) 880.
15. S. SUGANO and I. TSUJIKAWA, *ibid.* **13** (1958) 899.
16. Y. TANABE and S. SUGANO, *ibid.* **9** (1954) 753.
17. *Idem, ibid.* **9** (1954) 766.
18. F. DURVILLE *et al.*, *J. Phys. Chem. Solids* **6** (1985) 701.
19. F. J. BERGIN *et al.*, *J. Luminesc.* **34** (1986) 307.

Received 14 December 1988
and accepted 23 August 1989